Original Article

Diagnostic efficacy of cryobiopsy for peripheral pulmonary lesions with ground-glass opacity: a propensity score-matched analysis

Hideaki Furuse[1]^, Yuji Matsumoto[1,2]^, Toshiyuki Nakai[1]^, Midori Tanaka[1], Kanako Nishimatsu[1], Keigo Uchimura[1], Tatsuya Imabayashi[1], Takaaki Tsuchida[1]

[1]Department of Endoscopy, Respiratory Endoscopy Division, National Cancer Center Hospital, Tokyo, Japan; [2]Department of Thoracic Oncology, National Cancer Center Hospital, Tokyo, Japan

Contributions: (I) Conception and design: H Furuse, Y Matsumoto; (II) Administrative support: H Furuse, Y Matsumoto; (III) Provision of study materials or patients: All authors; (IV) Collection and assembly of data: H Furuse, Y Matsumoto, K Nishimatsu; (V) Data analysis and interpretation: H Furuse, Y Matsumoto; (VI) Manuscript writing: All authors; (VII) Final approval of manuscript: All authors.

Correspondence to: Yuji Matsumoto, MD, PhD. Department of Endoscopy, Respiratory Endoscopy Division, National Cancer Center Hospital, Tokyo, Japan; Department of Thoracic Oncology, National Cancer Center Hospital, 5-1-1 Tsukiji, Chuo-ku, Tokyo 1040045, Japan.
Email: yumatsum@ncc.go.jp.

Background: Peripheral pulmonary lesions (PPLs) with ground-glass opacity (GGO) are generally difficult to diagnose via bronchoscopy. Cryobiopsy, a recently introduced technique, provides quantitatively and qualitatively superior tissues compared with conventional biopsy methods and can improve diagnostic outcomes. However, its diagnostic accuracy has not been specifically investigated. Therefore, this study aimed to determine whether the combined use of cryobiopsy improves the diagnostic yield for PPLs with GGO.

Methods: Consecutive patients who underwent bronchoscopy combined with radial endobronchial ultrasound and virtual bronchoscopic navigation for PPLs with GGO were retrospectively reviewed between June 2014 and May 2020. Cryobiopsy was introduced at our institution in June 2017. Patients who underwent only conventional biopsy (forceps and/or needle aspiration) between June 2014 and May 2017 were classified as the conventional group, whereas those who underwent cryobiopsy with or without conventional biopsy between June 2017 and May 2020 were categorized as the "cryo" group. The diagnostic performance of the two groups was compared using propensity score-matched analysis.

Results: Overall, 553 cases were identified, including 250 and 303 in the cryo and conventional groups, respectively. Propensity scoring was implemented to match lesion characteristics and intraprocedural findings, leading to the selection of 232 pairs of cases for each matched (m) group. The diagnostic yield in the m-cryo group was significantly higher than that in the m-conventional group [88.8% *vs.* 63.8%, odds ratio: 4.50 (95% confidence interval: 2.76–7.33), P<0.001]. Although the incidence of grade 2 and 3 bleeding in the m-cryo group was higher than that in the m-conventional group (40.5% *vs.* 8.6% and 2.6% *vs.* 0.4%, respectively; P<0.001), grade 4 bleeding was not reported.

Conclusions: The combined use of cryobiopsy provides improved diagnostic yield for PPLs with GGO compared with conventional biopsy methods.

Keywords: Bronchoscopy; cryobiopsy; ground-glass opacity (GGO); peripheral pulmonary lesion (PPL)

Submitted Apr 07, 2024. Accepted for publication Jul 17, 2024. Published online Sep 12, 2024.
doi: 10.21037/tlcr-24-304
View this article at: https://dx.doi.org/10.21037/tlcr-24-304

^ ORCID: Hideaki Furuse, 0000-0002-9327-5155; Yuji Matsumoto, 0000-0003-0646-858X; Toshiyuki Nakai, 0000-0003-3223-5632.

Introduction

The detection of peripheral pulmonary lesions (PPLs), including those presenting with ground-glass opacity (GGO), has recently increased with the general use of low-dose computed tomography (CT) for the screening of lung cancer (1). PPLs with GGO have been reported in various diagnoses encompassing premalignant lesions, such as atypical adenomatous hyperplasia; malignant lesions, such as adenocarcinoma *in situ*; minimally invasive adenocarcinoma and invasive adenocarcinoma; and benign lesions, including focal interstitial fibrosis, aspergillosis, eosinophilic pneumonia, and organizing pneumonia (2). Persistent findings of GGO are frequently suggestive of neoplastic conditions with a high probability of malignancy, especially if the solid components are enlarged (3). However, ^{18}F-fluorodeoxyglucose-positron emission tomography is less effective in distinguishing malignant lesions from benign lesions in cases of PPLs with GGO than in those of solid PPLs (4). Therefore, it appears appropriate to have a histological diagnosis before surgery to formulate the best treatment plan for the patient.

Recently, several bronchoscopic devices, including radial endobronchial ultrasound (R-EBUS), virtual bronchoscopic navigation (VBN), and electromagnetic navigation bronchoscopy, have advanced diagnostic performance (5-10). However, diagnosing PPLs with GGO is more difficult than diagnosing solid PPLs, even with the use of these techniques (11,12), as PPLs with GGO exhibit relatively weak cellular atypia and/or poor invasion of the bronchial epithelium (13-15). Therefore, conventional biopsy techniques using forceps and/or aspiration needles are sometimes ineffective.

Highlight box

Key findings

- Cryobiopsy improves the diagnostic yield for peripheral pulmonary lesions (PPLs) with ground-glass opacity (GGO) compared with conventional biopsy methods.

What is known and what is new?

- PPLs with GGO are generally difficult to diagnose by bronchoscopy because they exhibit relatively weak cellular atypia and/or poor invasion of the bronchial epithelium.
- This propensity score-matched analysis revealed that cryobiopsy is associated with improved diagnostic yield for PPLs with GGO.

What is the implication, and what should change now?

- These findings have important implications for improving bronchoscopic diagnosis of PPLs with GGO.

Cryobiopsy, a recently introduced technique, provides high-quality tissue specimens in large volumes compared with forceps biopsy (16). Several studies have reported the utility of cryobiopsy specimens in diagnosing interstitial lung diseases (ILDs), which often present with GGO (17-19). In this context, we have frequently performed cryobiopsy for PPLs with GGO, assuming that it could improve the diagnostic outcome.

Our previous study, in which PPLs with GGO accounted for approximately half of the total cases, demonstrated that the addition of cryobiopsy improved the diagnostic outcome for PPLs compared with conventional biopsy methods (20) and that the diagnosis of PPLs with GGO tended to be more effective with cryobiopsy than that of solid PPLs. However, these findings just were based on a subgroup analysis of the study. Furthermore, GGO lesions range from pure ground-glass to part-solid with various ratios of solid components, making it difficult to simply compare their diagnostic performance. Hence, an additional study including only PPLs with GGO was considered necessary to prove the efficacy of cryobiopsy for the diagnosis of PPLs with GGO. The current study took into account the specific characteristics of GGO lesions and investigated whether cryobiopsy contributes to an improved diagnostic yield for PPLs with GGO compared with conventional biopsy methods. We present this article in accordance with the STROBE reporting checklist (available at https://tlcr.amegroups.com/article/view/10.21037/tlcr-24-304/rc).

Methods

Study subjects

Consecutive patients who underwent transbronchial biopsy for PPLs with GGO at our institution were retrospectively reviewed from June 2014 to May 2020. Cryobiopsy was introduced at our institution in June 2017. Patients who did not undergo cryobiopsy (between June 2014 and May 2017) were included in the conventional group, whereas those who underwent cryobiopsy (between June 2017 and May 2020) were included in the "cryo" group. Patients who did not undergo R-EBUS or VBN, those who did not undergo cryobiopsy between June 2017 and May 2020, and those who underwent a repeat biopsy for the same lesion were excluded from the analysis. The National Cancer Center Institutional Review Board approved this study (No. 2018-090), and individual consent for this retrospective analysis was waived. This study was conducted in accordance with

the Declaration of Helsinki (as revised in 2013).

Procedures

High-resolution CT (HRCT) with a slice thickness of ≤1.0 mm was performed before the bronchoscopy in all cases. PPL was characterized as a well-defined pulmonary lesion on HRCT that could not be directly observed by bronchoscopy. GGO was defined as a lesion with an attenuation area exhibiting a lower density than that of the surrounding vessels on HRCT without limitations on the ratio of solid components. The total size, solid component size, lobe, location, distance from the costal pleura, and bronchus sign were assessed on the axial HRCT. The total size and solid component size were determined using the longest diameter, and the distance from the costal pleura was defined as the shortest perpendicular length to the lateral border of the lesion. The consolidation tumor ratio (CTR) was calculated as the solid component size divided by the total size (21). Lesions located in the outer one-third of the hilum in the lung field on CT were classified as outer, whereas lesions located in the remaining regions were classified as inner, as defined by Baaklini *et al.* (22). If a bronchus led directly to the lesion, the bronchus sign was defined as positive. The visibility of the lesions was also evaluated using the corresponding chest radiography.

The majority of cases underwent the procedures on an outpatient basis. All procedures were conducted under local anesthesia with moderate to deep sedation using a combination of fentanyl or pethidine and midazolam or propofol. Bronchoscopes were selected from BF-P260F, BF-P290, BF-1T260, BF-1TQ290, and Y-0053 (23) (Olympus, Tokyo, Japan) at the operator's discretion. A Ziostation workstation (Ziostation2®; Ziosoft, Tokyo, Japan) was used to reconstruct VBN from the HRCT data (24). Once the bronchoscope reached the vicinity of the lesion, an R-EBUS probe (UM-S20-17S or UM-S20-20R, Olympus) was inserted under C-arm fluoroscopy. The detection of the R-EBUS probe in relation to the lesion was classified as "within", "adjacent to", or "invisible", as defined by Kurimoto *et al.* (5); the types of R-EBUS signals (blizzard, mixed blizzard, or solid) were also recorded (25). After R-EBUS probe was withdrawn, conventional biopsy (forceps biopsy and/or needle aspiration) was performed in the conventional group. All patients in the cryo group were intubated using an 8.0-mm inner diameter tracheal tube (Portex Uncuffed Ivory PVC, Oral/Nasal Tracheal Tube, Smiths Medical, Minneapolis, MN, USA) before the procedure, and conventional biopsy was performed, followed by cryobiopsy in most cases. The specimens were obtained using a 1.9-mm reusable cryoprobe (Erbe Elektromedizin GmbH, Tübingen, Germany) for cryobiopsy and frozen for 3–6 seconds. After withdrawing the specimen along with the bronchoscope, an auxiliary bronchoscope was promptly inserted to control subsequent bleeding (26-28). Rapid on-site cytological evaluation was performed in most cases. Cryobiopsy was performed once in most cases, with a maximum of two attempts in some cases.

Diagnosis

The diagnostic yield was defined as the number of diagnostic cases divided by the overall number of cases. Diagnostic cases were defined as malignant lesions with positive pathological features or benign lesions with specific pathological features compatible with the following surgical pathological or follow-up CT results for more than one year. The final diagnosis was determined based on the reports obtained through bronchoscopy, surgery, or follow-up CT findings (29). The final diagnosis was defined as unknown, and the case was classified as nondiagnostic in the following situations: (I) the bronchoscopic findings were not specific, and no following surgery was performed; (II) the bronchoscopic findings were inconsistent with follow-up CT results; or (III) the patient was lost to follow-up within one year of the bronchoscopy.

Adverse events

Data regarding complications were extracted for all adverse events during and after the bronchoscopic procedure. According to standardized definitions, bleeding was graded as follows: grade 0, none; grade 1, suctioning of blood required for <1 minute; grade 2, >1 minute of suctioning, repeat wedging of the bronchoscope, or instillation of cold saline, diluted vasoactive substances, or thrombin required for persistent bleeding; grade 3, selective intubation required for <20 minutes or premature interruption of the procedure; and grade 4, >20 minutes of persistent selective intubation or new admission to the intensive care unit or resuscitation (30). Chest radiography was performed to screen for pneumothorax if the patient reported dyspnea or chest pain after the bronchoscopy; however, this was not routinely performed.

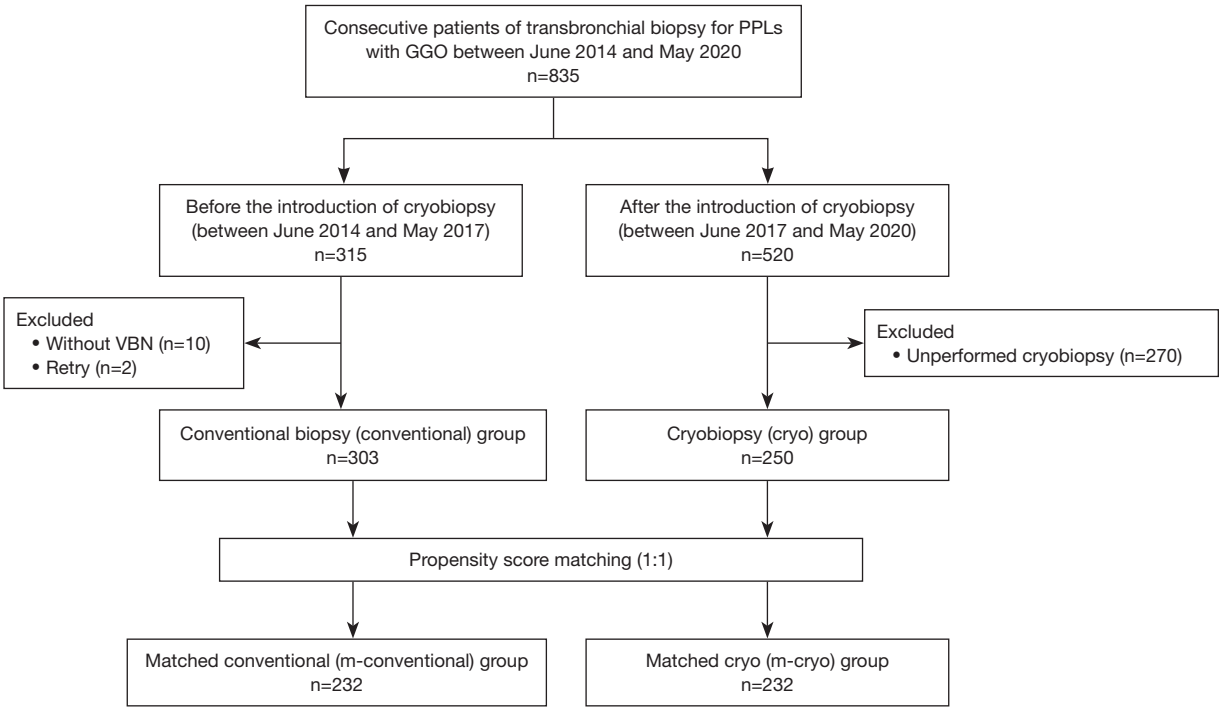

Figure 1 Flow diagram of patient selection. GGO, ground-glass opacity; PPL, peripheral pulmonary lesion; VBN, virtual bronchoscopic navigation.

Statistical analysis

Differences in the distribution of the baseline characteristics between the two groups were analyzed using Pearson's Chi-squared test or Fisher's exact test for categorical variables and the Mann-Whitney *U* test for continuous variables.

Propensity score-matched analysis was conducted to adjust for measurable confounders between the two groups. Multivariable logistic regression was used to predict the probability of undergoing cryobiopsy based on confounding covariates, age, sex, total size, CTR, lobe, location, distance from the costal pleura, bronchus sign, visibility on chest radiography, R-EBUS detection, and use of needle aspiration. Each case was assigned an estimated propensity score, which predicts the probability of undergoing cryobiopsy. One-to-one matching was used to select cases in the cryo and conventional groups with equivalent propensity scores to determine the diagnostic differences between the two groups. Univariable and multivariable logistic regression models were performed to determine diagnostic differences between the two groups after controlling for the characteristics of cases and intraprocedural findings. In addition, subgroup analysis was performed in the matched cohort using univariable logistic regression analysis based on lesion characteristics observed using CT and R-EBUS.

All statistical analyses were conducted using JMP® Pro 16.0.0 software (SAS Institute Inc., Cary, NC, USA), and two-sided P values of <0.05 were regarded as statistically significant.

Results

Among the 553 cases included in this study, 250 cases and 303 cases were assigned to the cryo and conventional groups, respectively (*Figure 1*). The lesions of the excluded patients, who did not undergo cryobiopsy after its introduction, tended to have a larger total size and high CTR. Moreover, these lesions involved the use of needle aspiration and were visible on chest radiography and classified as "within" by R-EBUS detection (Table S1).

The baseline characteristics of the included cases are presented in *Table 1*. The median (range) total sizes in the cryo and conventional groups were 22.3 (7.5–95.0) and 21.0 (6.0–64.7) mm, respectively (P=0.11), and the median CTRs were 0.53 (0–0.99) and 0.49 (0–0.99), respectively (P=0.31). In the overall cohort, the cryo group had a significantly better rate of R-EBUS detection (within: 56.8% *vs.* 53.8%;

Table 1 Baseline characteristics and clinical factors

Variable	Overall cases (n=553)			Propensity score-matched pairs (n=464)		
	Cryo group (n=250)	Conventional group (n=303)	P value	m-cryo group (n=232)	m-conventional group (n=232)	P value
Age (years)	69 [38–88]	69 [39–90]	0.86	70 [38–88]	69 [40–90]	0.83
Sex			>0.99			0.57
Male	104 (41.6)	125 (41.3)		97 (41.8)	90 (38.8)	
Female	146 (58.4)	178 (58.7)		135 (58.2)	142 (61.2)	
Total size (mm)	22.3 [7.5–95.0]	21.0 [6.0–64.7]	0.11	22.4 [7.5–95.0]	22.3 [6.0–64.7]	0.88
CTR	0.53 [0–0.99]	0.49 [0–0.99]	0.31	0.54 [0–0.99]	0.53 [0–0.99]	0.83
Lobe			0.98			0.88
RUL/LUS	141 (56.4)	173 (57.1)		129 (55.6)	133 (57.3)	
ML/lingula	30 (12.0)	35 (11.6)		27 (11.6)	28 (12.1)	
RLL/LLL	79 (31.6)	95 (31.4)		76 (32.8)	71 (30.6)	
Location			0.28			>0.99
Outer	191 (76.4)	219 (72.3)		175 (75.4)	175 (75.4)	
Inner	59 (23.6)	84 (27.7)		57 (24.6)	57 (24.6)	
Distance from the costal pleura (mm)	9.7 [0–50.4]	9.7 [0–53.9]	0.90	9.5 [0–50.4]	9.2 [0–53.9]	0.87
Bronchus sign			0.40			>0.99
Positive	201 (80.4)	234 (77.2)		185 (79.7)	186 (80.2)	
Negative	49 (19.6)	69 (22.8)		47 (20.3)	46 (19.8)	
Visibility on chest radiography			0.49			0.78
Visible	139 (55.6)	178 (58.7)		132 (56.9)	136 (58.6)	
Invisible	111 (44.4)	125 (41.3)		100 (43.1)	96 (42.4)	
R-EBUS detection			<0.001			>0.99
Within	142 (56.8)	163 (53.8)		133 (57.3)	133 (57.3)	
Adjacent to	106 (42.4)	117 (38.6)		97 (41.8)	97 (41.8)	
Invisible	2 (0.8)	23 (7.6)		2 (0.9)	2 (0.9)	
Use of needle aspiration			0.03			0.91
Yes	57 (22.8)	46 (15.2)		42 (18.1)	44 (19.0)	
No	193 (77.2)	257 (84.8)		190 (81.9)	188 (81.0)	

Values are presented as median [range] or number (%). The m-cryo and m-conventional groups are termed as such as these are propensity score-matched groups. CTR, consolidation tumor ratio; LLL, left lower lobe; LUS, left upper segment; ML, middle lobe; R-EBUS, radial endobronchial ultrasound; RLL, right lower lobe; RUL, right upper lobe.

adjacent to: 42.4% *vs.* 38.6%; and invisible: 0.8% *vs.* 7.6%, P<0.001) and a higher rate of needle aspiration use (22.8% *vs.* 15.2%, P=0.03) than the conventional group. No statistically significant differences were observed in the other evaluated factors. Notably, 79 and 109 cases in the cryo group and 100 and 115 cases in the conventional group showed blizzard signs and mixed blizzard signs on R-EBUS, respectively.

The propensity score-matched analysis yielded 232 pairs as the matched cryo (m-cryo) and conventional

Table 2 Final diagnostic results in the propensity score-matched cohort

Final diagnosis	m-cryo group (n=232)		m-conventional group (n=232)	
	Diagnostic	Nondiagnostic	Diagnostic	Nondiagnostic
Malignant				
Adenocarcinoma	196	19	141	62
Adenosquamous carcinoma	3	0	0	1
Squamous cell carcinoma	0	1	1	0
Pleomorphic carcinoma	0	0	1	0
Malignant lymphoma	1	0	0	0
MALT lymphoma	0	1	0	2
Metastatic tumor	1	0	2	0
Benign				
Organizing pneumonia	2	0	0	0
Inflammation	1	0	2	0
Granuloma	1	0	0	1
Fibrosis	0	0	0	1
Other benignity	1	0	1	2
Unknown	0	5	0	15

Values are presented as numbers. The m-cryo and m-conventional groups are termed as such as these are propensity score-matched groups. MALT, mucosa-associated lymphoid tissue.

(m-conventional) groups. After the matching, all clinical factors were favorably balanced between the two groups (*Table 1*). The final diagnosis in both groups was predominantly adenocarcinoma in the matched cohort (*Table 2*). Among those with adenocarcinoma as the final diagnosis, surgical resection was performed in 196 and 179 cases in the m-cryo and conventional groups, respectively. Among them, adenocarcinoma *in situ* and minimally invasive adenocarcinoma in surgical pathology were diagnosed in 5 and 15 cases in the m-cryo group and 5 and 14 cases in the m-conventional group, respectively.

The diagnostic yield was significantly higher in the m-cryo group compared with that in the m-conventional group {88.8% *vs.* 63.8%, odds ratio (OR): 4.50 [95% confidence interval (CI): 2.76–7.33], P<0.001} (*Table 3*). In the subgroup analysis, the use of cryobiopsy tended to be particularly effective for the lesions ≤20 mm in total size [OR: 5.96 (95% CI: 2.87–12.37)] and nonsolid lesions [OR: 8.54 (95% CI: 3.08–23.7)] (Table S2).

Large total size, high CTR, positive bronchus sign, good R-EBUS detection, and the use of cryobiopsy were identified as factors associated with a successful diagnosis in univariable and multivariable analyses, including all cases; visibility on chest radiography was identified as a factor in the univariable analysis only (*Table 4*).

As for complications, a higher number of grade 2/3 bleeding episodes were observed in the m-cryo group than in the m-conventional group (40.5% *vs.* 8.6% and 2.6% *vs.* 0.4%, respectively; P<0.001) (*Table 3*). However, there were no instances of grade 4 bleeding found in both groups. Most other adverse events were mild and, apart from bleeding, were comparable in the two groups. However, one patient in the m-cryo group had to be admitted due to cerebral infarction (24).

Discussion

The current study demonstrated that the use of cryobiopsy was related to a higher diagnostic yield for PPL with GGO via a specific evaluation of GGO lesions using a propensity score-matched analysis. In addition, the total size, CTR, bronchus sign, visibility on chest radiography, R-EBUS detection, and the use of cryobiopsy were identified as factors associated with a successful diagnosis.

Table 3 Diagnostic outcome and complications in the propensity score-matched cohort

Event	m-cryo group (n=232)	m-conventional group (n=232)	P value
Diagnostic outcome			
Diagnostic cases	206 (88.8)	148 (63.8)	<0.001
Complications			
Bleeding			<0.001
Grade 0/1	132 (56.9)	211 (90.9)	
Grade 2	94 (40.5)	20 (8.6)	
Grade 3	6 (2.6)	1 (0.4)	
Grade 4	0	0	
Other complications			
Pneumonia	0	1 (0.4)	
Pneumothorax	1 (0.4)	2 (0.8)	
Asthma exacerbation	1 (0.4)	0	
Cerebral infraction	1 (0.4)	0	

Values are presented as number (%). The m-cryo and m-conventional groups are termed as such as these are propensity score-matched groups.

Table 4 Clinical factors associated with successful diagnosis involving all cases

Variable	Reference	Univariable			Multivariable		
		Odds ratio	95% CI	P value	Adjusted odds ratio	95% CI	P value
Age (years)	Continuous	1.01	0.99–1.02	0.49	1.01	0.99–1.03	0.44
Male	Female	0.80	0.56–1.17	0.26	0.72	0.46–1.13	0.15
Total size (mm)	Continuous	1.07	1.05–1.10	<0.001	1.06	1.02–1.09	<0.001
CTR	Continuous	4.47	2.38–8.37	<0.001	3.61	1.64–7.97	0.002
Lesion in RUL/LUS	Lesion in ML/lingula	0.85	0.46–1.58	0.61	0.58	0.28–1.17	0.13
	Lesion in RLL/LLL	1.11	0.74–1.67	0.61	1.00	0.61–1.62	0.99
Outer location	Inner location	1.25	0.83–1.90	0.29	1.82	0.97–3.43	0.06
Distance from the costal pleura (mm)	Continuous	0.99	0.98–1.01	0.44	1.03	0.99–1.06	0.053
Positive bronchus sign	Negative bronchus sign	2.92	1.91–4.47	<0.001	1.87	1.10–3.17	0.02
Visible on chest radiography	Invisible on chest radiography	2.06	1.41–3.00	<0.001	1.07	0.64–1.80	0.79
R-EBUS detection “within”	R-EBUS detection “adjacent to”	1.69	1.14–2.50	0.009	1.79	1.14–2.81	0.01
	R-EBUS detection “invisible”	14.8	5.34–40.9	<0.001	5.26	1.78–15.5	0.003
Use of needle aspiration	Non-use of needle aspiration	1.27	0.77–2.08	0.35	1.14	0.63–2.05	0.66
Use of cryobiopsy	Non-use of cryobiopsy	5.42	3.46–8.50	<0.001	5.53	3.37–9.08	<0.001

The multivariable-adjusted model was adjusted for age, sex, total size, CTR, lobe, location, distance from the costal pleura, bronchus sign, visibility on chest radiography, R-EBUS detection, and the use of needle aspiration. CI, confidence interval; CTR, consolidation tumor ratio; LLL, left lower lobe; LUS, left upper segment; ML, middle lobe; R-EBUS, radial endobronchial ultrasound; RLL, right lower lobe; RUL, right upper lobe.

PPLs with GGO have a worse diagnostic outcome by transbronchial biopsy than solid PPLs (11,12). A previous study reported that the diagnostic OR of solid PPLs to PPLs with GGO was 2.30 (95% CI: 1.07–4.97) in multivariable analysis (12). One of the reasons is that PPLs with GGO tend to be less visible on radiography than solid PPLs (31). R-EBUS, an indispensable instrument for the detection of PPLs, can also be used for the detection of GGO lesions by focusing on the slight change that shows a hyperintense acoustic shadow (i.e., the so-called blizzard and mixed blizzard signs) (25). However, it is often difficult to guide the R-EBUS probe in the vicinity of PPLs with GGO because of their relatively poor visibility on radiography. Prior studies have reported that combining R-EBUS and VBN improved the diagnostic outcome of small PPLs and was especially effective in reaching invisible lesions on chest radiography (9,10). Therefore, using R-EBUS in combination with VBN is essential for the efficient detection of PPLs with GGO.

There are some barriers to the diagnosis of PPLs with GGO that are relevant to sampling, even with the use of R-EBUS and VBN. The diagnostic yield of transbronchial biopsy using forceps combined with R-EBUS, VBN, and fluoroscopy has been reported to be 47–69% for PPLs with GGO (12,32,33). These results are consistent with the diagnostic yield in the m-conventional group in the current study and demonstrate the limitations of diagnosing such lesions using forceps. The final diagnosis in the current study was adenocarcinoma in the majority of cases. In cases of early adenocarcinoma, tumor cells have poor invasion into the bronchial epithelium as they usually exhibit a lepidic growth pattern on the alveolar epithelium with weak cellular atypia (13-15), making it difficult to establish a definitive diagnosis using cytological specimens. Therefore, it is important to obtain tissues with a few crush artifacts that enable the evaluation of alveolar structure. Cryobiopsy has already been shown to be effective in diagnosing ILDs, including ground-glass appearance (17-19). The main characteristics of cryobiopsy specimens are that they are larger and less likely to be crushed than those collected via conventional biopsy. Therefore, these specimens can offer valuable information regarding the alveolar structures for diagnosing ILDs. This feature of cryobiopsy is also theoretically effective for the diagnosis of PPLs with GGO and is presumed to be the main reason why the m-cryo group had a higher diagnostic yield than the m-conventional group in the current study. A representative case that was diagnosed only with a specimen obtained via cryobiopsy is shown in *Figure 2*.

In the current study, total size, CTR, bronchus sign, visibility on chest radiography, R-EBUS detection, and the use of cryobiopsy were significantly associated with a successful diagnosis in univariable and multivariable analysis. Among these factors, CTR was newly identified as a diagnostic predictor, whereas the remaining factors have already been confirmed in previous studies (5-8,34). Previous research has demonstrated that lesions with a higher CTR are more pathologically suggestive of invasive adenocarcinoma (21). Thus, these lesions are more likely to invade the bronchial epithelium in addition to their better visibility on radiography and fluoroscopy, leading to easier and more streamlined diagnostic outcomes compared with those exhibiting a lower CTR.

Although reusable cryoprobes were used in the current study, single-use cryoprobes, which are more flexible, are frequently used in clinical practice at present. These single-use cryoprobes have already been reported to be useful in feasibility studies for small PPLs (35,36). Jiang *et al.* examined the diagnostic performance of the 1.1-mm single-use cryoprobe for PPLs with GGO and reported a diagnostic yield of 82.6% (37). Single-use cryoprobes are expected to facilitate the sampling of PPLs with various sites.

Regarding adverse events, the incidences of grade 2/3 bleeding were significantly higher in the cryo group than in the conventional group (40.5% *vs.* 8.6% and 2.6% *vs.* 0.4%, respectively, P<0.001). However, the risk of bleeding in cryobiopsy and conventional biopsy was comparable with the rates reported in our previous study, including all types of PPLs (38.0% *vs.* 10.2% and 1.5% *vs.* 0.8%, respectively, P<0.001) (20). In contrast, another study reported that cryobiopsy for PPLs with GGO had a significantly higher risk of bleeding than that for solid PPLs, with an OR of 9.30 (95% CI: 3.40–25.40) noted in multivariable analysis (27). In any case, it is important to take appropriate countermeasures to prevent bleeding when performing cryobiopsy for PPLs with GGO. The current study adopted the two-scope method as a countermeasure instead of using a bronchial blocker, as bronchial blockers may interfere with bronchoscopic manipulation when approaching small PPLs (25-27). No cases of grade 4 bleeding were observed in the current study, even without using a bronchial blocker. Thus, the two-scope method seems feasible for cryobiopsy even in patients with PPLs with GGO. However, it is also essential to avoid biopsy in areas with a high risk of bleeding. R-EBUS is able to detect not only the location of the lesion but

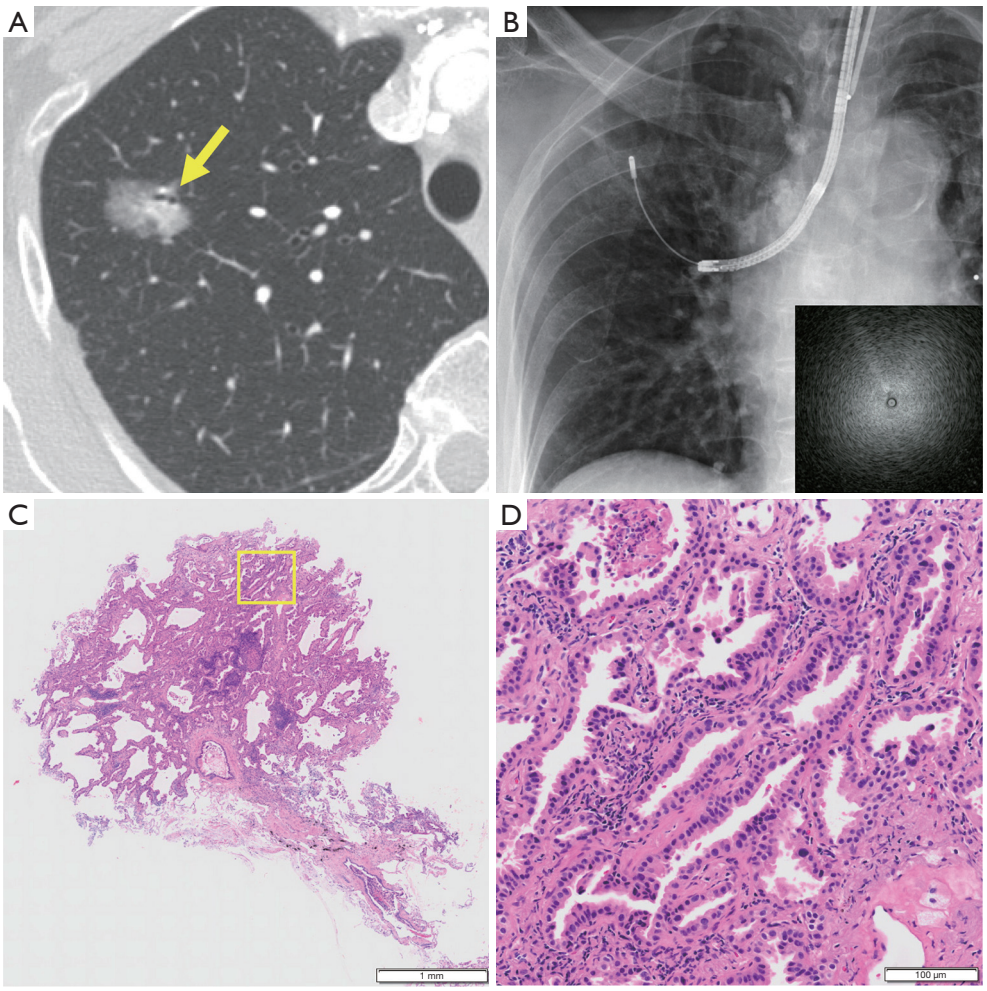

Figure 2 A representative case of a 69-year-old woman who could be diagnosed only with a specimen collected via cryobiopsy. (A) High-resolution CT shows a 22.5-mm part-solid nodule (arrow) in the right upper lobe with a positive bronchus sign. (B) Cryobiopsy was performed at the location where radial endobronchial ultrasound detected the lesion, which exhibited a blizzard sign (bottom right corner). (C) The specimen is 4.3 mm × 3.5 mm in size without noticeable crush artifacts (hematoxylin and eosin stain, ×1.2 magnification). (D) At higher magnification (square), tumor cells forming a lepidic growth pattern were clearly observed, leading to a diagnosis of adenocarcinoma (hematoxylin and eosin stain, ×10 magnification). CT, computed tomography.

also the presence of surrounding vessels. Thus, cryobiopsy should be avoided in areas where large surrounding vessels are detected by R-EBUS.

This study has some limitations. First, this was a retrospective, non-randomized study conducted at a single institution, and the time series of the cryo and conventional groups were different. Although the operators and detailed bronchoscopic procedures were somewhat different, it is unlikely that the time series had a meaningful impact on the results since key instruments other than the cryoprobe (i.e., R-EBUS and VBN) had already been established before the study period. Additionally, CT findings were evaluated by non-radiologists who were not blinded to the procedures, which could have potentially introduced bias. Second, cases in which cryobiopsy was not performed after its introduction were excluded. Such cases may have been biased toward a favorable diagnosis compared with those examined using cryobiopsy, making it reasonable to exclude them from the analysis given the difficulty in balancing confounders. Third, although propensity score-matched analysis was used to adjust for the characteristics of cases and intraprocedural findings, factors other than

those included in the propensity score calculation were not considered. Therefore, there may have been some cases in the m-conventional group in which it was difficult to conduct cryobiopsy. However, the results of this study should be considered reliable given the large number of enrolled cases and the inclusion of many factors relevant to the diagnosis via transbronchial biopsy in the regression models. Fourth, forceps biopsy and/or needle aspiration were performed, followed by cryobiopsy in most cases; thus, the diagnostic outcomes of the cryo group were not based solely on cryobiopsy alone. Conducting randomized controlled trials comparing cryobiopsy with conventional biopsy would be ideal to definitively demonstrate the efficacy of cryobiopsy for PPLs with GGO.

Conclusions

The present study demonstrates that the combined use of cryobiopsy improves the diagnostic yield of PPLs with GGO compared with conventional biopsy methods.

Acknowledgments

We thank Ryo Sadachi of the Division of Biostatistics, Center for Research Administration and Support, National Cancer Center, for providing advice on the statistical analyses.
Funding: This study was partially supported by the National Cancer Center Research and Development Fund (Nos. 29-A-13 and 2020-A-12).

Footnote

Reporting Checklist: The authors have completed the STROBE reporting checklist. Available at https://tlcr.amegroups.com/article/view/10.21037/tlcr-24-304/rc

Data Sharing Statement: Available at https://tlcr.amegroups.com/article/view/10.21037/tlcr-24-304/dss

Peer Review File: Available at https://tlcr.amegroups.com/article/view/10.21037/tlcr-24-304/prf

Conflicts of Interest: All authors have completed the ICMJE uniform disclosure form (available at https://tlcr.amegroups.com/article/view/10.21037/tlcr-24-304/coif). H.F. receives lecture fees from Erbe Elektromedizin GmbH and AstraZeneca. Y.M. receives a research funds from Hitachi; consulting fees from INTUITIVE; and lecture fees from Olympus, AstraZeneca, Novartis, COOK, AMCO, Thermo Fisher Scientific, Erbe Elektromedizin GmbH, Fujifilm, Chugai, Eli Lilly, Merck, Takeda, and ETHICON. K.U. receives grants from Japan Society for the Promotion of Science (JSPS) KAKENHI (Grant Number JP22K15698 and JP19K16966) and lecture fees from Novartis, Thermo Fisher Scientific, AstraZeneca, and Chugai. T.I. receives a research funds from Hitachi High-Tech Corporation and lecture fees from COOK, Chugai Pharma, Eli Lilly, Thermo Fisher Scientific K.K., Olympus, Novartis Pharma, and Fujifilm. The other authors have no conflicts of interest to declare.

Ethical Statement: The authors are accountable for all aspects of the work in ensuring that questions related to the accuracy or integrity of any part of the work are appropriately investigated and resolved. The study was conducted in accordance with the Declaration of Helsinki (as revised in 2013). This study was approved by The National Cancer Center's Institutional Review Board (No. 2018-090), and individual consent for this retrospective analysis was waived.

References

1. Yankelevitz DF, Yip R, Smith JP, et al. CT Screening for Lung Cancer: Nonsolid Nodules in Baseline and Annual Repeat Rounds. Radiology 2015;277:555-64.
2. Goo JM, Park CM, Lee HJ. Ground-glass nodules on chest CT as imaging biomarkers in the management of lung adenocarcinoma. AJR Am J Roentgenol 2011;196:533-43.
3. Kakinuma R, Noguchi M, Ashizawa K, et al. Natural History of Pulmonary Subsolid Nodules: A Prospective Multicenter Study. J Thorac Oncol 2016;11:1012-28.
4. Kim BT, Kim Y, Lee KS, et al. Localized form of bronchioloalveolar carcinoma: FDG PET findings. AJR

Am J Roentgenol 1998;170:935-9.
5. Kurimoto N, Miyazawa T, Okimasa S, et al. Endobronchial ultrasonography using a guide sheath increases the ability to diagnose peripheral pulmonary lesions endoscopically. Chest 2004;126:959-65.
6. Steinfort DP, Khor YH, Manser RL, et al. Radial probe endobronchial ultrasound for the diagnosis of peripheral lung cancer: systematic review and meta-analysis. Eur Respir J 2011;37:902-10.
7. Ali MS, Trick W, Mba BI, et al. Radial endobronchial ultrasound for the diagnosis of peripheral pulmonary lesions: A systematic review and meta-analysis. Respirology 2017;22:443-53.
8. Folch EE, Labarca G, Ospina-Delgado D, et al. Sensitivity and Safety of Electromagnetic Navigation Bronchoscopy for Lung Cancer Diagnosis: Systematic Review and Meta-analysis. Chest 2020;158:1753-69.
9. Ishida T, Asano F, Yamazaki K, et al. Virtual bronchoscopic navigation combined with endobronchial ultrasound to diagnose small peripheral pulmonary lesions: a randomised trial. Thorax 2011;66:1072-7.
10. Asano F, Shinagawa N, Ishida T, et al. Virtual bronchoscopic navigation combined with ultrathin bronchoscopy. A randomized clinical trial. Am J Respir Crit Care Med 2013;188:327-33.
11. Iwano S, Imaizumi K, Okada T, et al. Virtual bronchoscopy-guided transbronchial biopsy for aiding the diagnosis of peripheral lung cancer. Eur J Radiol 2011;79:155-9.
12. Okachi S, Imai N, Imaizumi K, et al. Factors Affecting the Diagnostic Yield of Transbronchial Biopsy Using Endobronchial Ultrasonography with a Guide Sheath in Peripheral Lung Cancer. Intern Med 2016;55:1705-12.
13. Takashima S, Maruyama Y, Hasegawa M, et al. Prognostic significance of high-resolution CT findings in small peripheral adenocarcinoma of the lung: a retrospective study on 64 patients. Lung Cancer 2002;36:289-95.
14. Aoki T, Tomoda Y, Watanabe H, et al. Peripheral lung adenocarcinoma: correlation of thin-section CT findings with histologic prognostic factors and survival. Radiology 2001;220:803-9.
15. Noguchi M, Morikawa A, Kawasaki M, et al. Small adenocarcinoma of the lung. Histologic characteristics and prognosis. Cancer 1995;75:2844-52.
16. Hetzel J, Hetzel M, Hasel C, et al. Old meets modern: the use of traditional cryoprobes in the age of molecular biology. Respiration 2008;76:193-7.
17. Hetzel J, Maldonado F, Ravaglia C, et al. Transbronchial Cryobiopsies for the Diagnosis of Diffuse Parenchymal Lung Diseases: Expert Statement from the Cryobiopsy Working Group on Safety and Utility and a Call for Standardization of the Procedure. Respiration 2018;95:188-200.
18. Maldonado F, Danoff SK, Wells AU, et al. Transbronchial Cryobiopsy for the Diagnosis of Interstitial Lung Diseases: CHEST Guideline and Expert Panel Report. Chest 2020;157:1030-42.
19. Raghu G, Remy-Jardin M, Richeldi L, et al. Idiopathic Pulmonary Fibrosis (an Update) and Progressive Pulmonary Fibrosis in Adults: An Official ATS/ERS/JRS/ALAT Clinical Practice Guideline. Am J Respir Crit Care Med 2022;205:e18-47.
20. Furuse H, Matsumoto Y, Nakai T, et al. Diagnostic efficacy of cryobiopsy for peripheral pulmonary lesions: A propensity score analysis. Lung Cancer 2023;178:220-8.
21. Suzuki K, Koike T, Asakawa T, et al. A prospective radiological study of thin-section computed tomography to predict pathological noninvasiveness in peripheral clinical IA lung cancer (Japan Clinical Oncology Group 0201). J Thorac Oncol 2011;6:751-6.
22. Baaklini WA, Reinoso MA, Gorin AB, et al. Diagnostic yield of fiberoptic bronchoscopy in evaluating solitary pulmonary nodules. Chest 2000;117:1049-54.
23. Sasada S, Izumo T, Chavez C, et al. A new middle-range diameter bronchoscope with large channel for transbronchial sampling of peripheral pulmonary lesions. Jpn J Clin Oncol 2014;44:826-34.
24. Matsumoto Y, Izumo T, Sasada S, et al. Diagnostic utility of endobronchial ultrasound with a guide sheath under the computed tomography workstation (ziostation) for small peripheral pulmonary lesions. Clin Respir J 2017;11:185-92.
25. Izumo T, Sasada S, Chavez C, et al. Radial endobronchial ultrasound images for ground-glass opacity pulmonary lesions. Eur Respir J 2015;45:1661-8.
26. Matsumoto Y, Nakai T, Tanaka M, et al. Diagnostic Outcomes and Safety of Cryobiopsy Added to Conventional Sampling Methods: An Observational Study. Chest 2021;160:1890-901.
27. Sriprasart T, Aragaki A, Baughman R, et al. A Single US Center Experience of Transbronchial Lung Cryobiopsy for Diagnosing Interstitial Lung Disease With a 2-Scope Technique. J Bronchology Interv Pulmonol 2017;24:131-5.
28. Nakai T, Watanabe T, Kaimi Y, et al. Safety profile and risk factors for bleeding in transbronchial cryobiopsy using

a two-scope technique for peripheral pulmonary lesions. BMC Pulm Med 2022;22:20.
29. Vachani A, Maldonado F, Laxmanan B, et al. The Impact of Alternative Approaches to Diagnostic Yield Calculation in Studies of Bronchoscopy. Chest 2022;161:1426-8.
30. Folch EE, Mahajan AK, Oberg CL, et al. Standardized Definitions of Bleeding After Transbronchial Lung Biopsy: A Delphi Consensus Statement From the Nashville Working Group. Chest 2020;158:393-400.
31. Tsubamoto M, Kuriyama K, Kido S, et al. Detection of lung cancer on chest radiographs: analysis on the basis of size and extent of ground-glass opacity at thin-section CT. Radiology 2002;224:139-44.
32. Nakai T, Matsumoto Y, Suzuk F, et al. Predictive factors for a successful diagnostic bronchoscopy of ground-glass nodules. Ann Thorac Med 2017;12:171-6.
33. Ikezawa Y, Shinagawa N, Sukoh N, et al. Usefulness of Endobronchial Ultrasonography With a Guide Sheath and Virtual Bronchoscopic Navigation for Ground-Glass Opacity Lesions. Ann Thorac Surg 2017;103:470-5.
34. Guvenc C, Yserbyt J, Testelmans D, et al. Computed tomography characteristics predictive for radial EBUS-miniprobe-guided diagnosis of pulmonary lesions. J Thorac Oncol 2015;10:472-8.
35. Tanaka M, Matsumoto Y, Imabayashi T, et al. Diagnostic value of a new cryoprobe for peripheral pulmonary lesions: a prospective study. BMC Pulm Med 2022;22:226.
36. Oki M, Saka H, Kogure Y, et al. Ultrathin bronchoscopic cryobiopsy of peripheral pulmonary lesions. Respirology 2023;28:143-51.
37. Jiang S, Liu X, Chen J, et al. A pilot study of the ultrathin cryoprobe in the diagnosis of peripheral pulmonary ground-glass opacity lesions. Transl Lung Cancer Res 2020;9:1963-73.

Cite this article as: Furuse H, Matsumoto Y, Nakai T, Tanaka M, Nishimatsu K, Uchimura K, Imabayashi T, Tsuchida T. Diagnostic efficacy of cryobiopsy for peripheral pulmonary lesions with ground-glass opacity: a propensity score-matched analysis. Transl Lung Cancer Res 2024;13(9):2175-2186. doi: 10.21037/tlcr-24-304

Supplementary

Table S1 Baseline characteristics and comparisons of clinical factors of patients who and did not undergo cryobiopsy after its introduction

Variable	Underwent cryobiopsy (n=250)	Did not undergo cryobiopsy (n=270)	P value
Age, years	69 [38–88]	71 [28–91]	0.17
Sex			0.60
Male	104 (41.6)	119 (44.1)	
Female	146 (58.4)	151 (55.9)	
Total size, mm	22.3 [7.5–95.0]	24.6 [8.4–93.8]	0.02
CTR	0.53 [0–0.99]	0.69 [0–0.99]	<0.001
Lobe			0.63
RUL/LUS	141 (56.4)	144 (53.3)	
ML/lingula	30 (12.0)	30 (11.1)	
RLL/LLL	79 (31.6)	96 (35.6)	
Location			0.76
Outer	191 (76.4)	204 (75.6)	
Inner	59 (23.6)	66 (24.4)	
Distance from the costal pleura, mm	9.7 [0–50.4]	7.8 [0–54.9)	0.14
Bronchus sign			0.24
Positive	201 (80.4)	205 (75.9)	
Negative	49 (19.6)	65 (24.1)	
Visibility on chest radiography			0.009
Visible	139 (55.6)	181 (67.0)	
Invisible	111 (44.4)	89 (33.0)	
R-EBUS detection			<0.001
Within	142 (56.8)	169 (62.6)	
Adjacent to	106 (42.4)	77 (28.5)	
Invisible	2 (0.8)	24 (8.9)	
Use of needle aspiration			0.048
Yes	57 (22.8)	83 (30.7)	
No	193 (77.2)	187 (69.3)	

Values are presented as median (range) or number (%). CTR, consolidation tumor ratio; LLL, left lower lobe; LUS, left upper segment; ML, middle lobe; R-EBUS, radial endobronchial ultrasound; RLL, right lower lobe; RUL, right upper lobe.

https://dx.doi.org/10.21037/tlcr-24-304

Table S2 Subgroup analysis in the matched cohort

Subgroup	Diagnostic cases		Odds ratio	95% CI	P value
	m-cryo group	m-conventional group			
Overall	206/232 (88.8)	148/232 (63.8)	4.50	2.76–7.33	<0.001
Total size					
≤20 mm	73/85 (85.9)	48/95 (50.5)	5.96	2.87–12.37	<0.001
>20 mm	133/147 (90.5)	100/137 (73.0)	3.52	1.80–6.85	<0.001
CTR					
CTR =0	37/45 (82.2)	13/37 (35.1)	8.54	3.08–23.7	<0.001
0< CTR ≤0.5	58/66 (87.9)	51/75 (68.0)	3.41	1.41–8.26	<0.001
0.5< CTR	111/121 (91.7)	84/120 (70.0)	4.75	2.23–10.13	<0.001
R-EBUS detection					
Within	124/133 (93.2)	94/133 (70.7)	5.71	2.64–12.38	<0.001
Adjacent to	81/97 (83.5)	54/97 (55.7)	4.03	2.06–7.87	<0.001

Values are presented as number (%). The m-cryo and m-conventional groups are termed as such as these are propensity score-matched groups. CI, confidence interval; CTR, consolidation tumor ratio; R-EBUS, radial endobronchial ultrasound.

https://dx.doi.org/10.21037/tlcr-24-304